

## Supplementary Information

### An Eco-Friendly Adhesive with Ultra-Strong Adhesive Performance

Zhenyu Yang,<sup>\*[a]</sup> Xiaoting Ji,<sup>[a]</sup> Xin-long Sha,<sup>[a]</sup> Jincheng Ding,<sup>[a]</sup> Lin Cheng,<sup>[b]</sup>  
Guangfeng Li<sup>\*[c,d]</sup>

[a] Prof. Z. Yang<sup>\*</sup>, X. Ji, Dr. X. Sha, Dr. J. Ding

School of Chemical and Environmental Engineering, Yancheng Teachers University,  
Yancheng City 224007, P. R. China

E-mail: yangzy@yctu.edu.cn

[b] Dr. L. Cheng

School of Chemistry and Chemical Engineering, Shanghai Jiao Tong University,  
Shanghai 200240, P. R. China

[c] Prof. G. Li<sup>\*</sup>

Department of Chemistry, Stoddart Institute of Molecular Science, Zhejiang  
University, Hangzhou 310058, P. R. China

E-mail: guangfengli@zju.edu.cn

[d] Prof. G. Li<sup>\*</sup>

Zhejiang-Israel Joint Laboratory of Self-Assembling Functional Materials, ZJU-  
Hangzhou Global Scientific and Technological Innovation Center, Zhejiang University,  
Hangzhou 311215, P. R. China

## Table of contents

<b>1. Materials</b>	<b>S3</b>
<b>2. Preparation of the adhesive CBAX</b>	<b>S3</b>
<b>3. Characterization of the adhesive CBAX</b>	<b>S3</b>
<b>4. Multi-reuse experiments</b>	<b>S5</b>
<b>5. Solvent resistance experiments</b>	<b>S5</b>
<b>6. Statistical analysis</b>	<b>S6</b>
<b>7. Reference</b>	<b>S13</b>

## 1. Materials

All the reagents and solvents were obtained and used without further purification. Thiocetic acid (TA, 97%) was purchased from Shanghai Adamas-Beta Co. Ltd., tris(2-aminoethyl)amine (TREN, 98%) was purchased from Bide Pharmatech Co. Ltd. All other reagents were bought from commercial sources and used without any purification unless stated.

## 2. Preparation of the Adhesive CBAX

**Preparation of CBAX.** Taking the preparation of CBA0.6 as an example, TA (1.0 g, 4.9 mmol) was charged into a 50 mL flask and heated at 120 °C for 0.5 hours, then TREN (4.3 g, 2.9 mmol) was added. The reaction mixture was further stirred at 120 °C for another 4 hours. Subsequently, the reaction system was placed in a vacuum drying oven at 100°C under vacuum for 12 hours to remove the free water molecules formed during the reaction. The prepared adhesive was directly used for adhesion and other tests without further purification or separation.

**Table S1.** The content and ratio (mol %) of CBAX

	CBA0.2	CBA0.4	CBA0.6	CBA0.8	CBA1.0
TA	83.3	71.4	62.5	55.6	50
TREN	16.7	28.6	37.5	44.4	50

## 3. Characterization of the adhesive CBAX

**<sup>1</sup>H Nuclear Magnetic Resonance.** <sup>1</sup>H NMR spectra were required at room temperature using a Bruker Advance III HD 400 MHz NMR spectrometer (Germany) using the deuterated solvent as the lock and the residual solvent or TMS as the internal reference.

**The Thermal Behaviors Test.** Thermogravimetric analysis (TGA) was conducted using a TA Q500 (TA Instruments, New Castle, Delaware, USA) under a

stable nitrogen gas flow. Each sample was heated from 30-800 °C with a heating rate of 10 °C min<sup>-1</sup>. Differential scanning calorimeter (DSC) measurements were carried out using a TA Q200 (TA Instruments, New Castle, Delaware, USA), from -50 to 150°C at a rate of 10 °C/min in a nitrogen atmosphere. The glass transition temperatures ( $T_g$ ) was analyzed by utilizing a heat/cool/heat cycle with about 10 mg sample. In the cyclic thermal measurement, these samples were first heated from 25 to 100 °C and kept for 5min to eliminate the possible impacts from the thermal history, then cooled to -50 °C and reheated to 150 °C,  $T_g$  was determined in the second heat cycle.

**Rheology Behaviors Test.** The rheological behavior of CBA0.6 was assessed using a rheometer (AR2000, TA Instrument, USA) equipped with parallel plate geometry (25 mm diameter). Throughout the experimental procedure, the gap distance was maintained at 0.5 mm. Master curves of storage modulus ( $G'$ ) and loss modulus ( $G''$ ) were obtained by time-temperature superposition shifts at a reference temperature of 60 °C. Based on the Arrhenius plot of temperature-dependent shift factors, apparent activation energy ( $E_a$ ) was calculated from the slope of the curve. The temperature sweeps were performed from 35 to 100 °C for CBA0.6 with a heating rate of 5 °C/min under the frequency of 1.0 rad/s. Stress relaxation measurements were carried out under the strain amplitude of 1% at 50 °C, 60 °C, and 70 °C.

**Lap-Shear Adhesion Test.** Lap shear tests were conducted using an INSTRON 68TM-5 universal testing machine with a 20 mm/min strain rate at room temperature or -196 °C. The adhesive, approximately 36 mg/cm<sup>2</sup>, was applied to two identical substrates measuring 50 mm × 20 mm × 0.9 mm, with an overlap area of 200 mm<sup>2</sup> (20 mm × 10 mm). Two paper clips held the substrates together, and two stainless steel wires with a thickness of approximately 0.15 mm were used to control the adhesive thickness during heating. Thermal treatment was conducted in an oven at 100 °C for 30 min. Before the lap shear test, the bonded sheets were cooled to room temperature and allowed to stand for another 12 hours. Shear adhesion strength was determined by dividing the maximum force at joint failure by the overlapping contact area. Each set of sample data underwent a minimum of five tests, and the results were averaged for accuracy.

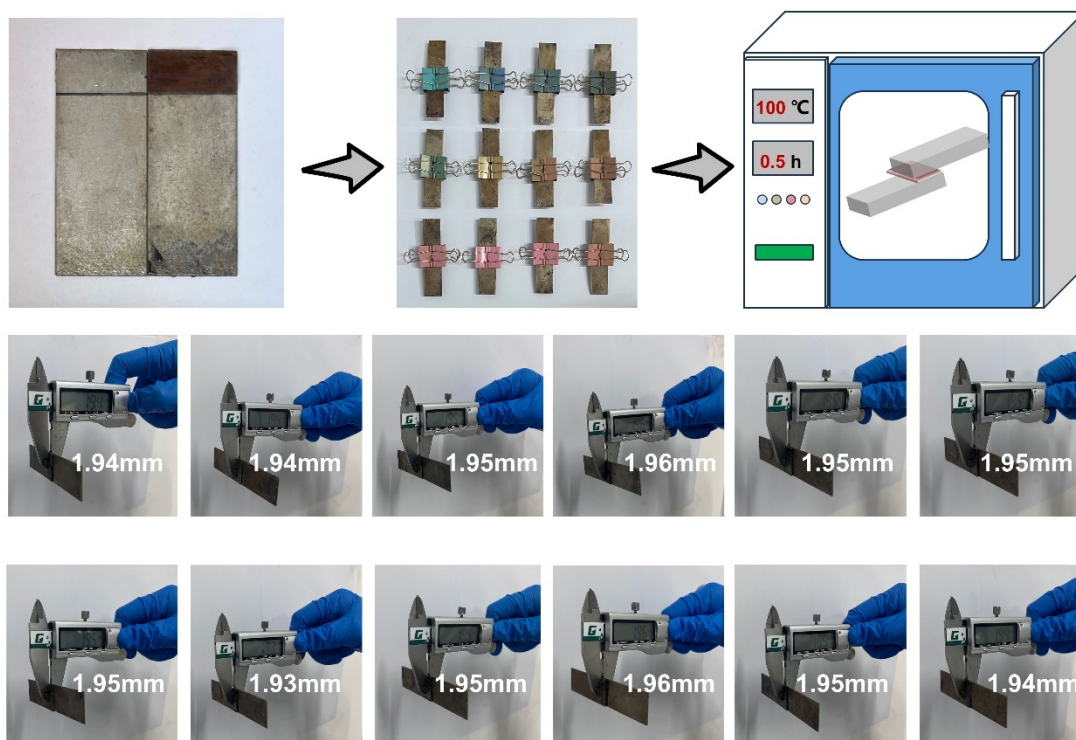


**Figure S1.** The sample preparation process for lap shear tests.

#### **4. Multi-reuse experiments**

Prepare a suitable amount of the adhesive CBA0.6 and use it entirely for lap shear tests on iron sheets (with more than five samples), taking the average value as the first cycle. After testing, recover all the adhesive, heat and remold it, and perform lap shear tests again with more than five samples, taking the average value as the second cycle. Repeat this process. As the adhesive CBA0.6 is reused more times, its hardness increases, requiring higher temperatures for hot pressing. By the tenth cycle, at least 150 °C is needed for hot pressing. To avoid the carbonization of the adhesive, we believe that ten cycles represent the upper limit of CBA0.6's reuse lifespan.

#### **5. The solvent resistance experiments**

The solvent resistance test involves immersing iron bonded with the adhesive CBA0.6 in different solvents for 24 hours, then air drying naturally for 12 hours before directly using for lap shear tests.

## 6. Statistical analysis

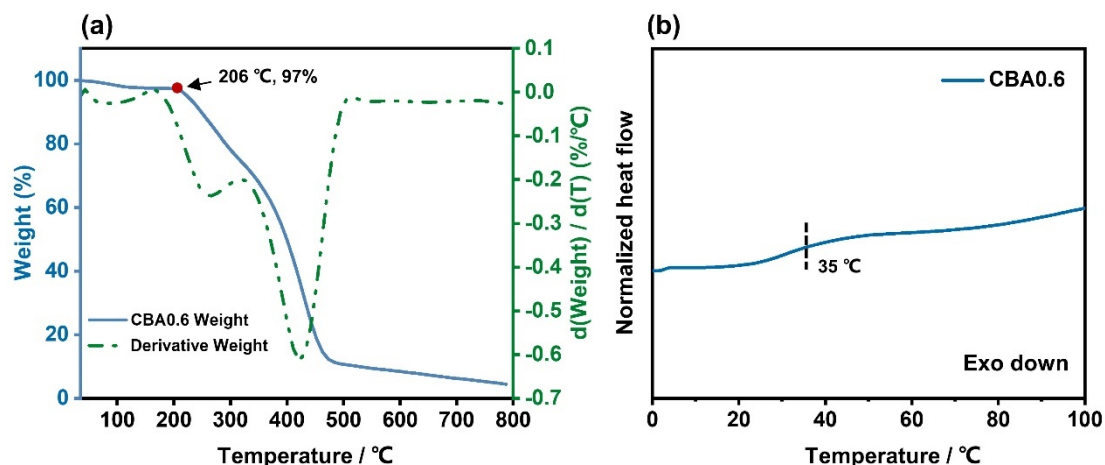


**Figure S2.** (a) Thermogravimetric analysis (TGA) curve of CBA0.6 under N<sub>2</sub> flow with 10 °C/min ramp rate. (b) Differential scanning calorimeter (DSC) measurement of CBA0.6 was performed at 10 °C/min in a nitrogen atmosphere.

$$\ln a_T = \frac{E_a}{R} \left( \frac{1}{T} - \frac{1}{T_{ref}} \right) \quad \text{Equation S1}$$

The relationship between the horizontal shift factor ( $a_T$ ) obtained from the master curve of CBA0.6 and its corresponding test temperature is shown in Fig. 3d. The results demonstrate that  $a_T$  is significantly dependent on temperature. When the temperature exceeds 60 °C, the relationship follows the Arrhenius equation (Equation S1), By fitting the  $a_T$  values, the activation energy ( $E_a$ ) of CBA0.6 is calculated to be approximately 270 kJ/mol, which is slightly higher than the disulfide bond energy of 251 kJ/mol. This value is slightly higher than the disulfide bond energy of 251 kJ/mol due to the presence of crosslinking networks. The high activation energy indicates the rapid scission of disulfide bonds at elevated temperatures and leads to a transition between the glassy and liquid states. In other words, the viscosity of CBA0.6 decreases rapidly within a narrow temperature range, demonstrating its excellent processing performance.

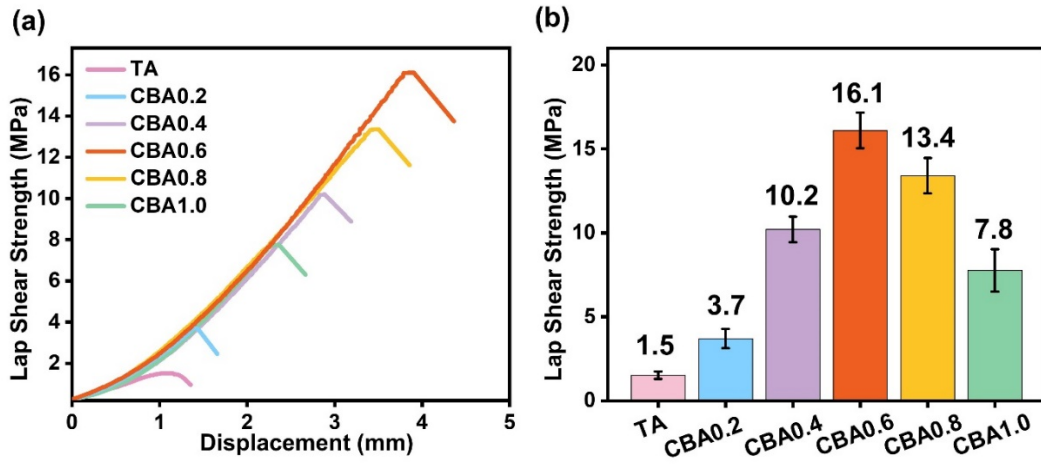


**Figure S3.** Assessment of the adhesive properties of bioadhesives CBAx. (a) and (b) are lap shear strength-displacement curves and lap shear strengths of adhesive CBAx. Error bars show the standard deviation of the measured adhesion strengths and Young's modulus of the CBAx ( $n \geq 5$ ).

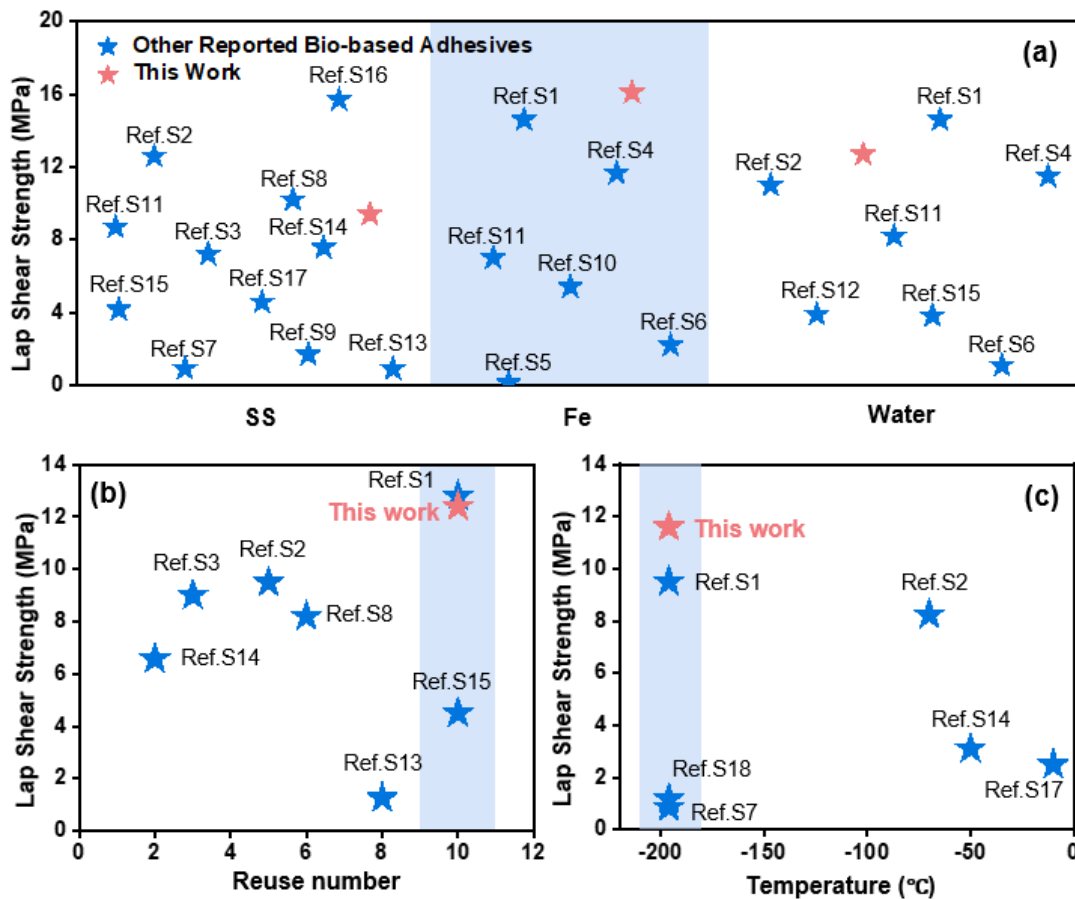


**Figure S4.** The bonding strength comparison of CBA0.6 with reported adhesives. (a) The adhesive strength in bonding with SS, Fe, and underwater performance. (b) The adhesion strengths of reuse numbers. (c) The adhesive strength at low temperature.

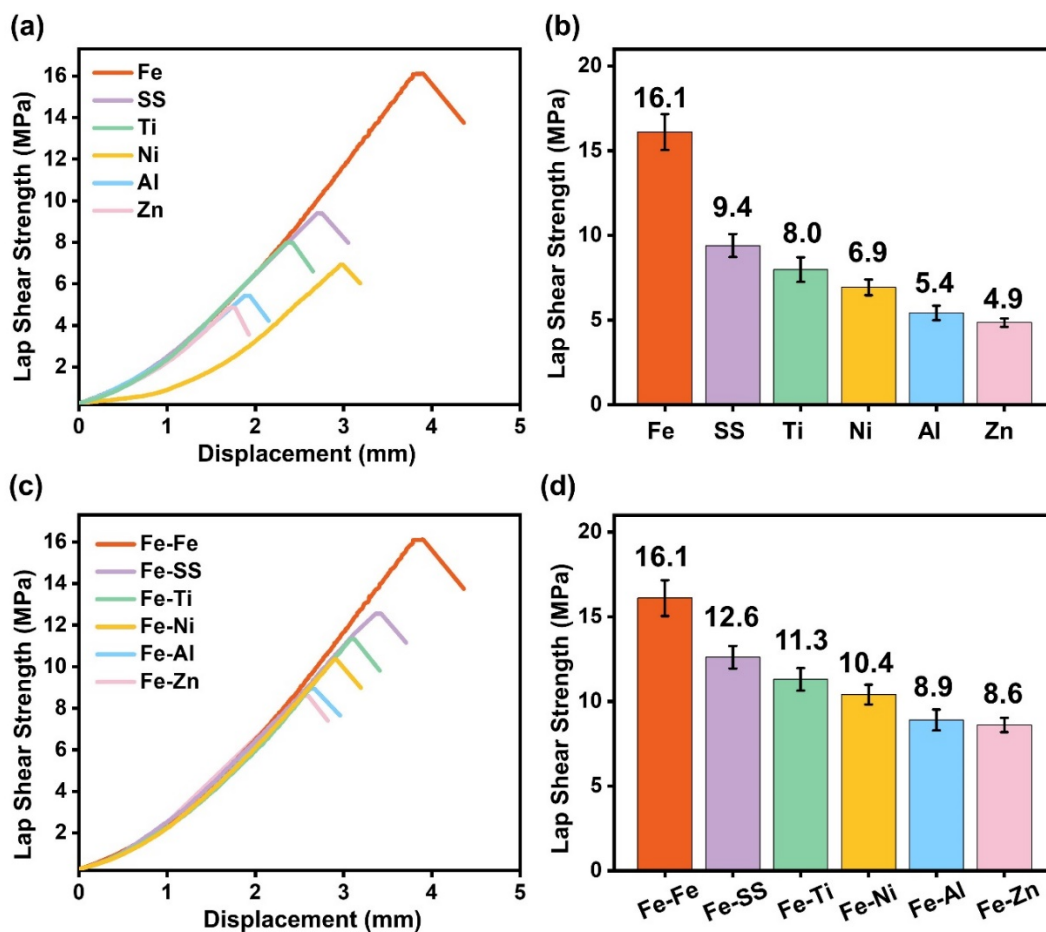


**Figure S5.** The adhesion testing of CBA0.6 to various materials. (a) and (b) present lap shear strength-displacement curves and corresponding lap shear strengths of CBA0.6 when bonding Fe, SS, Ti, Ni, Al, and Zn. (c) and (d) depict lap shear strength-displacement curves and lap shear strengths of CBA0.6 when bonding Fe with Fe, SS, Ti, Ni, Al, and Zn. Error bars show the standard deviation of the measured adhesion strengths of CBA0.6 ( $n \geq 5$ ).

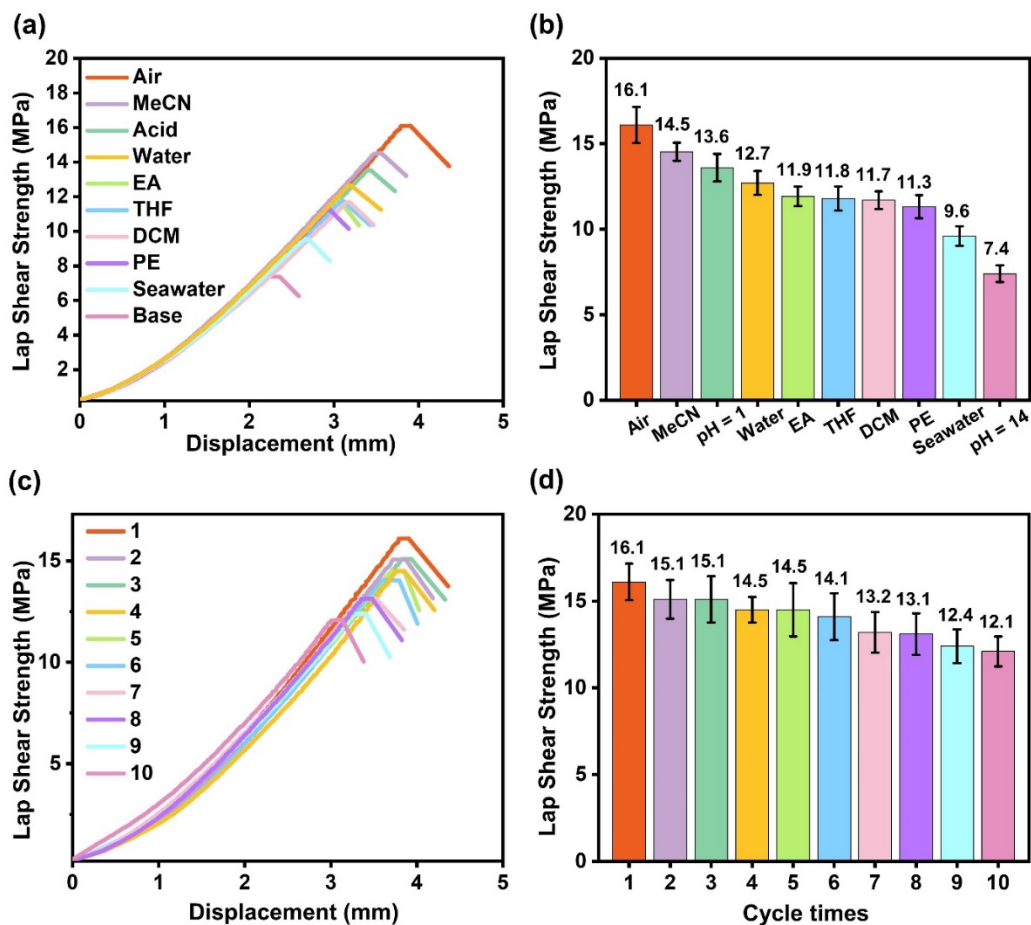


**Figure S6.** The solvent resistance and reusability of CBA0.6. (a) and (b) present lap shear strength-displacement curves and lap shear strengths of CBA0.6 when bonding Fe specimens immersed in various solvents for 24 hours, including MeCN, Acid (pH=1), Water, EA, THF, DCM, PE, Seawater, Base (pH=14). (c) and (d) depict lap shear strength-displacement curves and lap shear strengths of CBA0.6 in bonding Fe specimens after each reuse cycle. Error bars show the standard deviation of the measured adhesion strengths of CBA0.6 ( $n \geq 5$ ).

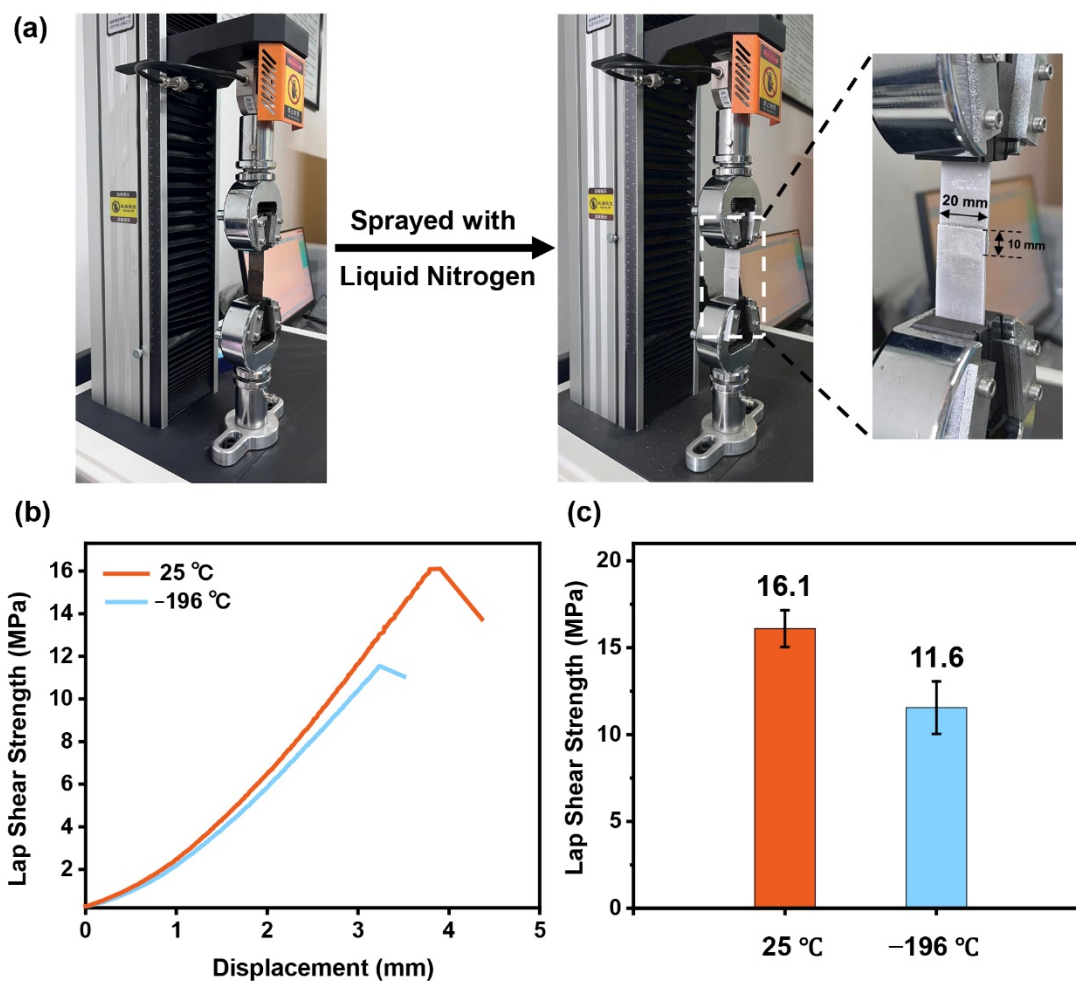


**Figure S7.** The anti-freezing property test of CBA0.6. (a) The digital image of lap shear tests performed at  $-196\text{ }^{\circ}\text{C}$ . (c) and (d) Strength-displacement curves and lap shear strengths of CBA0.6 at room temperature and  $-196\text{ }^{\circ}\text{C}$ . Error bars show the standard deviation of the measured adhesion strengths of CBA0.6 ( $n \geq 5$ ).

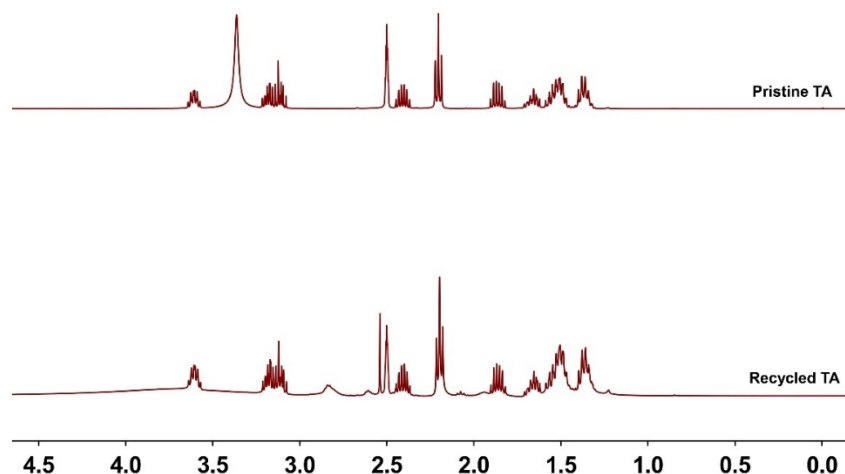


**Figure S8.**  $^1\text{H}$  NMR (400 MHz, DMSO) of full spectra of pristine and recycled TA.

As shown in Figure S8, the primary difference between the  $^1\text{H}$  NMR spectra of the pristine TA and the recycled TA lies in the appearance of distinct peaks. Specifically, the pristine TA exhibits an additional peak at 3.3 ppm, while the recycled TA shows a prominent single peak at 2.54 ppm. The 3.3 ppm peak in the pristine TA is attributed to residual water in deuterated DMSO. Upon recycling, the addition of deuterated TFA induces hydrogen-deuterium exchange with water molecules, resulting in the disappearance of the water peak. Conversely, the single peak at 2.54 ppm in the recycled TA corresponds to residual DMSO. This arises from the degradation process of CBA0.6, which involves a substantial amount of DMSO and TFA. Given the high boiling point of DMSO, trace amounts of this solvent are retained in the recycled TA.

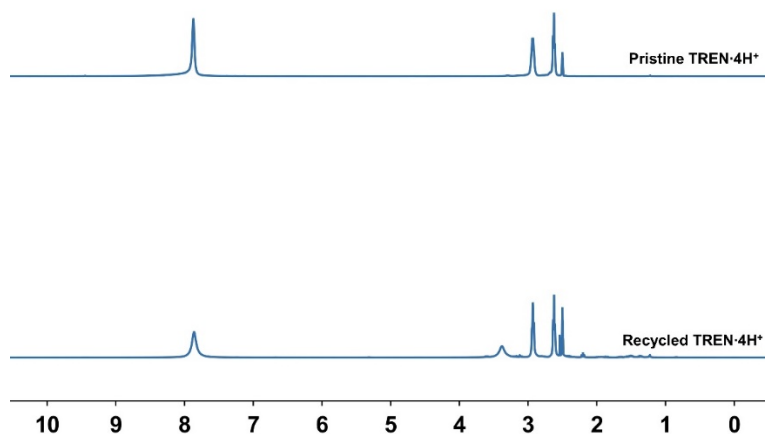


**Figure S9.**  $^1\text{H}$  NMR (400 MHz, DMSO) of full spectra of pristine and recycled TREN-4H $^+$ .

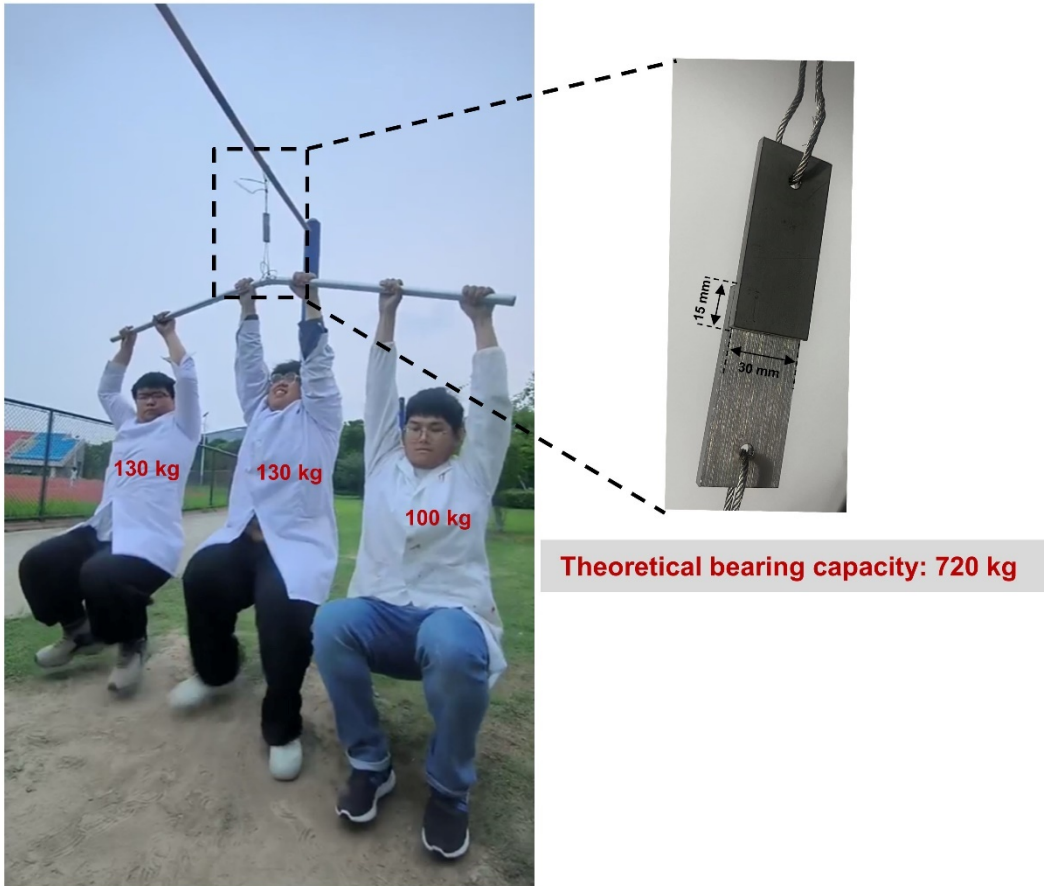


**Figure S10.** The digital image depicts CBA0.6 bonded iron sheets lifting three adults with a combined weight of approximately 360 kg. The bonding area is 450 mm<sup>2</sup>, and the theoretical bearing capacity is 720 kg.

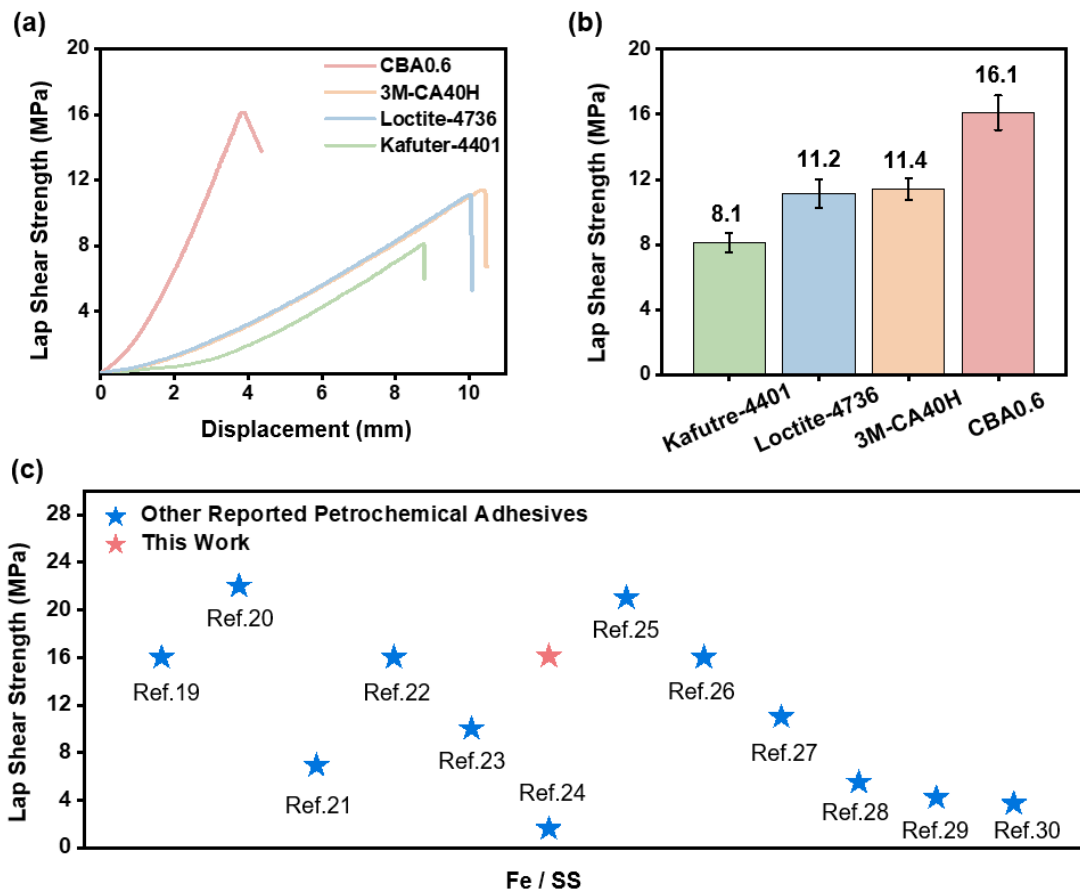


**Figure S11.** Comparison of the performance of CBA0.6 and petrochemical adhesives. (a) and (b) Lap shear strengths of CBA0.6 and commercial adhesives, including Kafuter-4404, Loctite-4736, and 3M-CA40H. (c) Comparative analysis of the lap shear strength of CBA0.6 with that of petrochemical adhesives recently reported in high-impact journals.

## 7. Reference

1. C. Heinzmann, U. Salz, N. Moszner, G. L. Fiore, C. Weder, *ACS Appl. Mater. Interfaces*. 2015, **7**, 13395–13404.
2. C. L. Jenkins, H. M. Siebert, J. J. Wilker, *Macromolecules* 2017, **50**, 561–568.
3. Q. Zhang, C.-Y. Shi, D.-H. Qu, Y.-T. Long, B. L. Feringa, H. Tian, *Sci. Adv.* 2018, **4**, eaat8192.
4. N. Moini, M. Khaghanipour, K. Kabiri, A. Salimi, M. J. Zohuriaan-Mehr, A. Jahandideh, *ACS Sustainable Chem. Eng.* 2019, **7**, 16247–16256.
5. S. Wu, C. Cai, F. Li, Z. Tan, S. Dong, *CCS Chem.* 2020, **3**, 1690–1700.
6. X. Li, J. Lai, Y. Deng, J. Song, G. Zhao, S. Y. Dong, *J. Am. Chem. Soc.* 2020, **142**, 21522–21529.
7. X. Li, Y. Deng, J. Lai, G. Zhao, S. Dong, *J. Am. Chem. Soc.* 2020, **142**, 5371–5379.
8. P. Sun, Y. Li, B. Qin, J.-F. Xu, X. Zhang, *ACS Mater. Lett.* 2021, **3**, 1003–1009.
9. Y. Yao, Z. Xu, B. Liu, X. Meng, J. Yang, W. Liu, *Adv. Funct. Mater.* 2021, **31**, 2006944.
10. J. Zhang, Z. Chen, Y. Zhang, S. Y. Dong, Y. Chen, S. Zhang, *Adv. Mater.* 2021, **33**, 2100962.
11. P. Sun, S. Mei, J.-F. Xu, X. Zhang, *Adv. Sci.* 2022, **9**, 2203182.
12. X. Xie, X. Xu, Y. Jiang, *ACS Appl. Polym. Mater.* 2022, **4**, 4319–4328.
13. Z. Wang, Y. Wang, H. Wang, H. Gang, N. Zhang, Y. Zhou, S. Gu, Y. Zhuang, W. Xu, G. Ke, Z. Li, H. Yang, *ACS Appl. Mater. Interfaces*. 2023, **15**, 24846–24857.
14. K. Wu, M. Fu, Y. Zhao, E. Gerhard, Y. Li, J. Yang, J. Guo, *Bioact. Mater.* 2023, **20**, 93–110.
15. C. Cui, Y. Sun, X. Nie, X. Yang, F. Wang, W. Liu, *Adv. Funct. Mater.* 2023, **33**, 2307543.

16. H. Gao, X. Wu, J. Fan, Z. Wang, *ACS Sustainable Chem. Eng.* 2024, **12**, 2668–2677.
17. R. Qie, S. Z. Moghaddam, E. Thormann, *ACS Sustainable Chem. Eng.* 2024, **12**, 4456–4463.
18. H. S. Wang, S. H. Gao, Y. T. Xie, X. Y. Shi, C. H. Lai, D. H. Lai, C. P. Wang, F. X. Chu, *ACS Appl. Polym. Mater.* 2024, DOI: 10.1021/acsapm.4c00129.
19. C. J. Higginson, K. G. Malollari, Y. Xu, A. V. Kelleghan, N. G. Ricapito, P. B. Messersmith, *Angew. Chem. Int. Ed.* **2019**, *58*, 12271.
20. X. Li, Y. Deng, J. Lai, G. Zhao, S. Dong, *J. Am. Chem. Soc.* **2020**, *142*, 5371.
21. R. Cheng, L. Yin, Y. Wen, B. Zhai, Y. Guo, Z. Zhang, W. Liao, W. Xiong, H. Wang, S. Yuan, J. Jiang, C. Liu, J. He, *Nat. Commun.* **2022**, *13*, 5241.
22. K. Zhao, Y. Liu, Y. Ren, B. Li, J. Li, F. Wang, C. Ma, F. Ye, J. Sun, H. Zhang, K. Liu, *Angew. Chem. Int. Ed.* **2022**, *61*, e202207425.
23. Z.-H. Wang, B.-W. Liu, F.-R. Zeng, X.-C. Lin, J.-Y. Zhang, X.-L. Wang, Y.-Z. Wang, H.-B. Zhao, *Sci. Adv.* **2022**, *8*, eadd8527.
24. W. Guan, W. Jiang, X. Deng, W. Tao, J. Tang, Y. Li, J. Peng, C.-L. Chen, K. Liu, Y. Fang, *Angew. Chem. Int. Ed.* **2023**, *62*, e202303506.
25. C. R. Westerman, B. C. McGill, J. J. Wilker, *Nature* **2023**, *621*, 306.
26. P. Niu, C. Li, J. Zhu, Y. Zhao, Z. Li, A. Sun, L. Wei, K. Wu, Y. Li, *Angew. Chem. Int. Ed.* **2024**, *63*, e202408840.
27. J. Fan, C. Ju, S. Fan, X. Li, Z. Zhang, N. Hadjichristidis, *Angew. Chem. Int. Ed.* **2024**, e202418764.
28. J. Feng, Z. Lin, Y. Zhang, L. Fang, Q. Zhu, D. Yu, *Angew. Chem. Int. Ed.* **2024**, *63*, e202411815.
29. K. Liu, P. Wu, *Angew. Chem. Int. Ed.* **2024**, *63*, e202403220.

30. X. Xie, Y. Jiang, X. Yao, J. Zhang, Z. Zhang, T. Huang, R. Li, Y. Chen, S.-L. Li, Y-Q. Lan, *Nat. Commun.* **2024**, *15*, 5017.